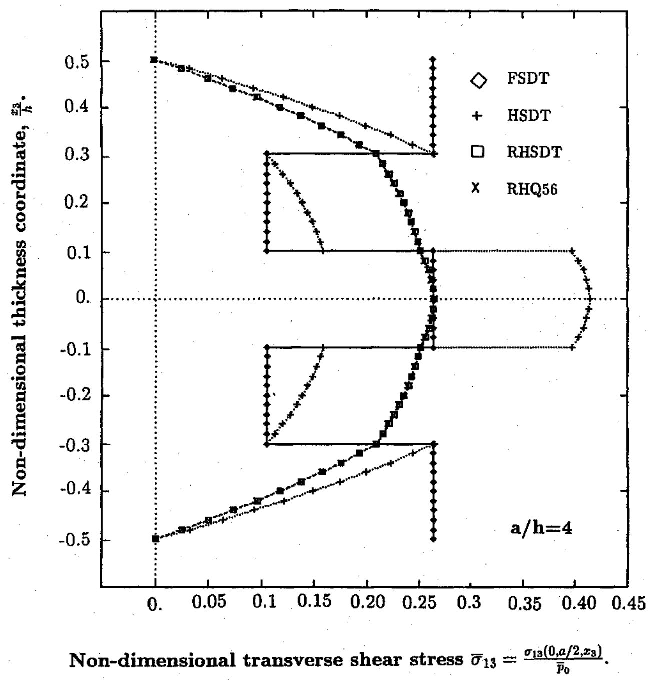

Fig. 2 Thickness-wise distribution of the nondimensional transverse shear stress in a five-layered symmetric cross-ply (0/90/0/90/0) square plate under bisinusoidal loading, as obtained from constitutive equations. Analytical and finite element method results.

HSDT [RHSDT]) with those predicted by the exact elasticity solution[6] and other commonly used bidimensional plate models: FSDT and HSDT. The quoted results refer to the cylindrical bending problem in the (x_1, x_3) plane. This sample problem has been investigated for purpose of comparison with exact elasticity solutions.[6] It is remarkable the very good correlation existing between the estimates of the RHSDT plate model and the exact elasticity solution. On the contrary, notice the inadequacy of all smeared plate models to give acceptable prediction for this quantity. Figure 2 refers to the bending of a square plate and compares analytical and finite element results. Because of symmetry, only one quarter of the plate has been modeled with 5×5 plate elements. All of the results were obtained by using the Gauss quadrature formula with 5×5 integrating points. Notice the high accuracy of the developed plate element. It should be remarked that numerical tests not reproduced here for sake of brevity show that 1) when compared with third-order plate modeling (HSDT), which will not fulfill the continuity stress conditions at the interfaces, the proposed third-order zig-zag approach also improves the prediction of the through-thickness distributions of the in-plane response (in-plane displacements and stresses) and 2) this plate element is practically locking free and behaves well also in distorted configurations.

It is concluded that the proposed approach gives very accurate results for low plate thickness ratios and high relative values of the elastic moduli and does not require any arbitrary shear correction factor. It is of importance to remember that the thickness-wise distributions were obtained from the lamina constitutive equations. It is the authors' opinion that the most important numerical advantage of the third-order zig-zag approach is in the finite element formulation, because continuous thickness-wise distributions of the transverse shear stresses can be obtained without resorting to the integration of the local equilibrium equations. In effect, the last approach requires second derivatives of the displacement field, thus lowering the accuracy of the approximation.

References

[1]Di Sciuva, M., "Multilayered Anisotropic Plate Models with Continuous Interlaminar Stresses," *Composite Structures*, Vol. 22, No. 3, 1992, pp. 149–168.

[2]Di Sciuva, M., "A Generalization of the Zig-Zag Plate Models to Account for General Lamination Configurations," *Atti Accademia delle Scienze di Torino-Classe di Scienze Fisiche, Matematiche e Naturali*, Vol. 28, Fasc. 3–4, 1994, pp. 81–103.

[3]Di Sciuva, M., "A General Quadrilateral Multilayered Anisotropic Plate Element with Continuous Interlaminar Stresses," *Computers and Structures*, Vol. 47, No. 1, 1993, pp. 91–105.

[4]Di Sciuva, M., Icardi, U., and Dobrynin, V., "An Eight Noded Multilayered Plate Element Based on a Refined Discrete-Layer Plate Theory," *Proceedings of the XII Congresso Nazionale AIDAA* (Como, Italy), Italian Association of Aeronautics and Astronautics, Milan, Italy, 1993, pp. 1023–1034.

[5]Di Sciuva, M., "A Third-Order Triangular Multilayered Plate Finite Element with Continuous Interlaminar Stresses," *International Journal for Numerical Methods in Engineering*, Vol. 38, No. 1, 1995, pp. 1–26.

[6]Pagano, N. J., "Exact Solutions for Rectangular Bidirectional Composites and Sandwich Plates," *Journal of Composite Materials*, Vol. 4, Jan. 1970, pp. 20–34.

Ribbed Cylindrical Shells Under a Concentrated Transverse Load

Sıddık Şener*
Gazi University, Ankara 06571, Turkey

Introduction

IN this Note, a circular cylindrical shell is assumed to be simply supported. The material behavior of the shell and the rib is linearly elastic, and the material is homogeneous and isotropic. The solution of a ribbed shell under a concentrated load is obtained by considering the shell and the rib separately. The interaction forces, which arise along the contact line between the rib and the shell are expanded in Fourier series, and then the solutions of the ring and the shell under the interaction forces are obtained. The unit displacement matrix is used with the boundary conditions, which gives the unknown amplitudes of the interaction forces. Thus, knowing these amplitudes, the displacements under the loads are obtained from the ring or from the isotropic shell. In this way the analytic solution of the ribbed shell is accomplished. At the end of this Note, a numerical example is discussed and the solution is summarized in the figures and table.

Formulation of the Ribbed Shell

The ends of the shell (Fig. 1) are assumed to be supported with diaphrams (not shown in the figure) that are very rigid in their plane and flexible out of the plane, so that the shell can be considered to be simply supported.

After all parameters of the problem are expressed in Fourier series, the equilibrium equations of the shell are

$$[\Phi]_m \{X\}_m = \{X_0\}_m \tag{1}$$

The unit displacement matrix $[\Phi]$ of the total system includes the rib $[\theta]$ and the isotropic shell $[\Phi_1]$ unit displacement matrices,

$$([\Phi_1] + [\theta])_m \{X\}_m = \{X_0\}_m \tag{2}$$

This expression can be written in the form

$$\left[\begin{bmatrix} w_r & w_t \\ v_r & v_t \end{bmatrix}_{sh} + \begin{bmatrix} w_r & w_t \\ v_r & v_t \end{bmatrix}_{rg} \right]_m \begin{Bmatrix} X_1 \\ X_2 \end{Bmatrix}_m = \begin{Bmatrix} w_0 \\ v_0 \end{Bmatrix}_{sh,m} \tag{3}$$

The unknown quantities X_1 and X_2 denote the amplitudes of the interaction forces and are obtained from Eq. (3). The displacements

Received June 2, 1993; revision received Feb. 4, 1995; accepted for publication Feb. 20, 1995.

*Professor, Department of Civil Engineering.

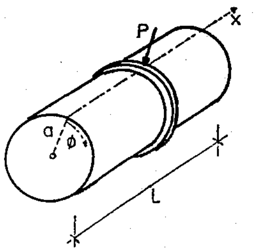

Fig. 1 Simply supported ribbed shell; supports and reactions are not shown.

in axial, tangential, and radial directions (u, v, w) under the load are found from the shell or from the ring equations

$$\begin{Bmatrix} w \\ v \end{Bmatrix} = \sum_{m=2}^{\infty} \left\{ \begin{bmatrix} w_r & w_t \\ v_r & v_t \end{bmatrix}_{sh} \begin{Bmatrix} X_1 \\ X_2 \end{Bmatrix}_m - \begin{Bmatrix} w_0 \\ v_0 \end{Bmatrix}_{sh} \right\}$$
$$= -\sum_{m=2}^{\infty} \begin{bmatrix} w_r & w_t \\ v_r & v_t \end{bmatrix}_{rg} \begin{Bmatrix} X_1 \\ X_2 \end{Bmatrix}_m \tag{4}$$

where the r, t, and 0 subscripts indicate the radial, tangential, and external load influence, respectively. The stress resultants of the ribbed shell are obtained by using the shell equations:

$$\begin{Bmatrix} M_x \\ M_\phi \\ \vdots \\ Q_\phi \\ N_{\phi x} \end{Bmatrix} = \sum_{m=2}^{\infty} \left\{ \begin{bmatrix} M_{xr} & M_{xt} \\ M_{\phi r} & M_{\phi t} \\ \vdots & \vdots \\ Q_{\phi r} & Q_{\phi t} \\ N_{\phi xr} & N_{\phi xt} \end{bmatrix} \begin{Bmatrix} X_1 \\ X_2 \end{Bmatrix} - \begin{Bmatrix} M_{x0} \\ M_{\phi 0} \\ \vdots \\ Q_{\phi 0} \\ N_{\phi x0} \end{Bmatrix} \right\}_m \tag{5}$$

where m is an integer. M_x, M_ϕ, Q_x, Q_ϕ, $N_{x\phi}$, $N_{\phi x}$ are the bending moments, the transverse shearing, and the shearing forces in the axial and circumferential directions, respectively. When the number of harmonics increases, the solution will approach the exact result. The harmonic for $m = 1$ and the resultants of tangential for $m = 0$ are excluded because the associated interaction forces are not self-equilibrating.

Solution of the Simply Supported Ribbed Shell

The displacement and stress resultants of the shell and the ring are needed under the radial and tangential interaction loads. The displacement and stress resultants in the circumferential direction under the radial and tangential interaction forces are obtained in accordance with Flügge's equations (see Refs. 1–3). Interaction forces or any external load may be represented by the periodic functions, such as the Fourier series. The displacements, and the stress resultants of the shell are expressed in the same series form as

$$u = u_m \cos m\phi; \qquad v = v_m \sin m\phi$$
$$w = w_m \cos m\phi; \qquad M_\phi = M_{\phi m} \cos m\phi \tag{6}$$
$$N_{x\phi} = N_{x\phi m} \sin m\phi; \qquad Q_x = Q_{xm} \cos m\phi$$

When these quantities in Eq. (6) are substituted in shell equilibrium equations, three simultaneous differential equations are obtained. The prime indicates the partial derivative with respect to x:

$$u_m'' - \frac{1-\mu}{2} m^2 u_m + \frac{1+\mu}{2} m v_m' + \mu w_m'$$
$$-k\left(\frac{1-\mu}{2} m^2 u_m + w_m''' + \frac{1-\mu}{2} m^2 w_m'\right) = 0 \tag{7a}$$

$$-\frac{1+\mu}{2} m u_m' - m^2 v_m + \frac{1-\mu}{2} v_m'' - m w_m$$
$$+k\left[\frac{3}{2}(1-\mu) v_m'' + \frac{3-\mu}{2} m w_m''\right] = 0 \tag{7b}$$

$$\mu u_m' + m v_m + w_m + k\left(-\frac{1-\mu}{2} m^2 u_m' - u_m''' - \frac{3-\mu}{2} m v_m''\right.$$
$$\left. + w_m'''' - 2m^2 w_m'' + m^4 w_m - 2m^2 w_m + w_m\right) = 0 \tag{7c}$$

where $k = t^2/12a^2$ is constant and a, t, and L are the radius, thickness, and length of the shell, respectively. If the solution of the shell equations (7) are chosen as exponential functions having constant coefficients,

$$u_m = A e^{sx/a}, \qquad v_m = B e^{sx/a}, \qquad w_m = C e^{sx/a} \tag{8}$$

they can have a solution different from zero only if the determinant formed from their nine coefficients vanishes. This condition leads to an eight-degree equation:

$$s^8 - 2(2m^2 - \mu)s^6 + \left[\frac{1-\mu^2}{k} + 6m^2(m^2-1)\right]s^4 - 2m^2$$
$$\times [2m^4 - (4-\mu)m^2 + (2-\mu)]s^2 + m^4(m^2-1)^2 = 0 \tag{9}$$

The eight roots are

$$s_1 = -y_1 + iz_1; \qquad s_2 = -y_1 - iz_1$$
$$s_3 = -y_2 + iz_2; \qquad s_4 = -y_2 - iz_2 \tag{10a}$$

$$s_5 = y_1 + iz_1; \qquad s_6 = y_1 - iz_1$$
$$s_7 = y_2 + iz_2; \qquad s_8 = y_2 - iz_2 \tag{10b}$$

The complete solution is the sum of all roots, with eight independent sets of constants A_j, B_j, and C_j:

$$p1 = y_1 x/a \tag{11a}$$
$$q1 = z_1 x/a \tag{11b}$$
$$p2 = y_2 x/a \tag{11c}$$
$$q2 = z_2 x/a \tag{11d}$$

$$u_m = e^{-p1}\left(A_1 e^{iq1} + A_2 e^{-iq1}\right) + e^{-p2}\left(A_3 e^{iq2} + A_4 e^{-iq2}\right)$$
$$+ e^{p1}\left(A_5 e^{iq1} + A_6 e^{-iq1}\right) + e^{p2}\left(A_7 e^{iq2} + A_8 e^{-iq2}\right) \tag{11e}$$

$$v_m = e^{-p1}\left(B_1 e^{iq1} + B_2 e^{-iq1}\right) + e^{-p2}\left(B_3 e^{iq2} + B_4 e^{-iq2}\right)$$
$$+ e^{p1}\left(B_5 e^{iq1} + B_6 e^{-iq1}\right) + e^{p2}\left(B_7 e^{iq2} + B_8 e^{-iq2}\right) \tag{11f}$$

$$w_m = e^{-p1}\left(C_1 e^{iq1} + C_2 e^{-iq1}\right) + e^{-p2}\left(C_3 e^{iq2} + C_4 e^{-iq2}\right)$$
$$+ e^{p1}\left(C_5 e^{iq1} + C_6 e^{-iq1}\right) + e^{p2}\left(C_7 e^{iq2} + C_8 e^{-iq2}\right) \tag{11g}$$

The constants A_j, B_j, and C_j are linearly dependent. Therefore, A_j and B_j can be expressed in terms of C_j, that is,

$$A_j = \alpha_j C_j; \qquad B_j = \beta_j C_j \tag{12}$$

Consider the three components of the displacements of the simply supported shell: displacement along the generator u must be symmetric, and the circumferential displacement v and the radial displacement w must be antisymmetric with respect to a central ring. These conditions yield displacement equations for four unknown constants:

$$w_m = C_2 \cosh p1 \sin q1 - C_1 \sinh p1 \cos q1$$
$$+ C_4 \cosh p2 \sin q2 - C_3 \sinh p2 \cos q2 \tag{13a}$$

$$v_m = (\beta_1 C_2 - \beta_2 C_1) \cosh p1 \sin q1 - (\beta_1 C_1 + \beta_2 C_2)$$
$$\times \sinh p1 \cos q1 + (\beta_3 C_4 - \beta_4 C_3) \cosh p2 \sin q2$$
$$- (\beta_3 C_3 + \beta_4 C_4) \sinh p2 \cos q2 \tag{13b}$$

$$u_m = (\alpha_1 C_1 + \alpha_2 C_2) \cosh p1 \cos q1 - (\alpha_1 C_2 - \alpha_2 C_1)$$
$$\times \sinh p1 \sin q1 + (\alpha_3 C_3 + \alpha_4 C_4) \cosh p2 \cos q2$$
$$- (\alpha_3 C_4 - \alpha_4 C_3) \sinh p2 \sin q2 \tag{13c}$$

These unknown constants are found from the boundary conditions which are written on the ring (Fig. 2). The boundary conditions for the radial line loads applied to the circumferential direction (Fig. 2a) at $x = L/2$.

$$N_{x\phi} = 0; \qquad Q_x = R/2; \qquad u = 0; \qquad w' = 0 \tag{14}$$

The boundary conditions for the tangential line loads applied to the circumferential direction (Fig. 2b) at $x = L/2$

$$N_{x\phi} = T/2; \qquad Q_x = 0; \qquad u = 0; \qquad w' = 0 \tag{15}$$

where R and T are the radial and tangential interaction loads, respectively. With the help of boundary conditions which are written in the circumferential direction, the solution of the shell subjected to interaction loads is obtained. The general form of the stress resultants can be written as follows for the symmetric group:

$$\begin{aligned} g = c[(a_1C_1 + a_2C_2)\cosh p1 \cos q1 - (a_1C_2 - a_2C_1) \\ \times \sinh p1 \sin q1 + (a_3C_3 + a_4C_4)\cosh p2 \cos q2 \\ - (a_3C_4 - a_4C_3)\sinh p2 \sin q2] \cos(\sin) m\phi \end{aligned} \tag{16a}$$

and for the antisymmetric group:

$$\begin{aligned} g = -c[(a_1C_1 + a_2C_2)\sinh p1 \cos q1 - (a_1C_2 - a_2C_1) \\ \times \cosh p1 \sin q1 + (a_3C_3 + a_4C_4)\sinh p2 \cos q2 \\ - (a_3C_4 - a_4C_3)\cosh p2 \sin q2] \cos(\sin) m\phi \end{aligned} \tag{16b}$$

Table 1 Displacements and stress resultants in ribbed shell

Displacement: Stress resultants:	w/f	M_x/P	M_ϕ/P	tN_x/P	tN_ϕ/P
Smooth shell	−31.32	0.257	0.243	−0.153	−0.203
	(31.02)	(0.238)	(0.245)	(0.151)	(0.204)
Ribbed shell	−11.67	0.035	0.030	−0.065	−0.106

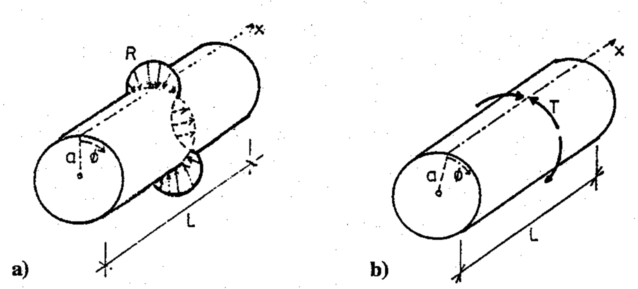

Fig. 2 Line load: a) radial and b) tangential, applied at $x = L/2$.

The coefficients c, a_1, and a_2 for the various displacements and stress resultants, are given in Table 1 of Ref. 1.

The ring is investigated under the influence of radial and circumferential interaction loads.[1,4] Displacements and stress resultants are obtained for the ring. After analyses of the ring and the shell have been completed, the solution of the ribbed shell can be obtained from Eqs. (1–5).

Example

Reconsider the simply supported shell under a concentrated transverse load applied to reinforcing ring (Fig. 1). The numerical analysis is illustrated in this example of a hinged cylindrical shell reinforced by one frame member and subjected to a concentrated load.[5] The twisting and bending of the frame in the plane tangent to the middle plane will be disregarded. A ribbed shell reinforced by symmetrically arranged rib (Fig. 1) with the following parameters was considered:

$$a/t = 30, \qquad L/a = 1.5, \qquad I/(bta^2) = 0.0115$$

$$A/(bt) = 5.0, \qquad S/(bt) = 0, \qquad f = P/(Et)$$

$$\mu = 0.3, \qquad b/t = 1.0$$

where P is the concentrated force applied to the shell, μ is Poisson's ratio, E is Young's modulus, and b, A, S, and I are the width, area, static moment, and moment inertia, respectively, of ring according to shell surface. Because of the symmetry of the shell in both the

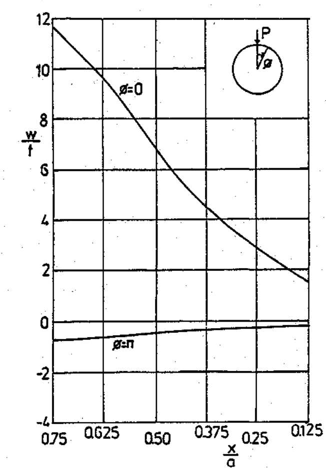

Fig. 4 Radial displacement of ribbed shell.

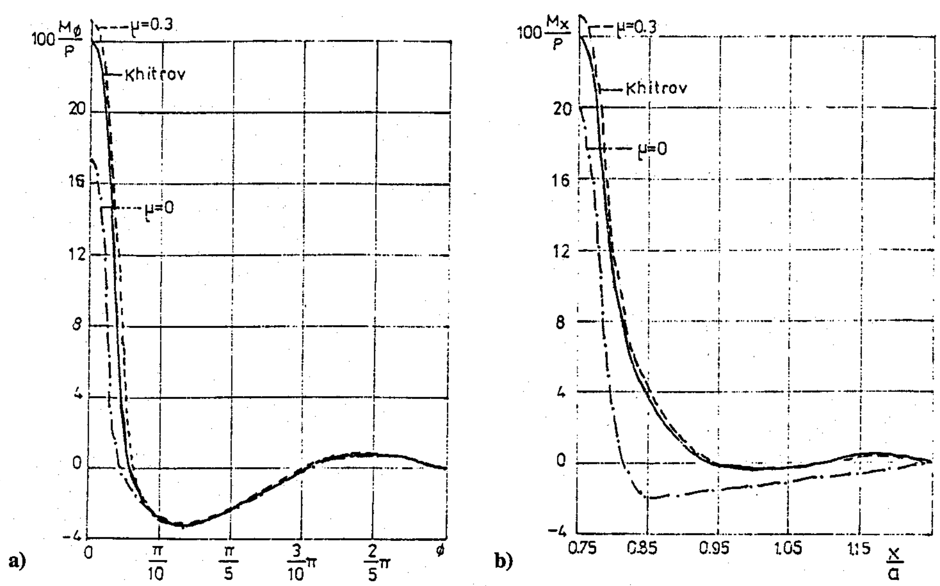

Fig. 3 M_ϕ and M_x moments for smooth shell: a) at midspan and b) for $\phi = 0$.

longitudinal and circumferential directions, solutions are obtained for a quarter shell. The same dimensions are used for a smooth shell; the variations of M_ϕ and M_x are given in Fig. 3, where the dashed lines represent the corresponding variations for a smooth shell.

Displacement and stress resultants under the load are given in Table 1 for $m = 41$. The results taken from Ref. 6 are given in parentheses. The radial displacements of the ribbed shell are plotted in Fig. 4.

Conclusions

To obtain sufficiently accurate figures for deflections, only a small number of significant terms is required. But the number of significant terms required to ensure a similar degree of accuracy for bending moments is much larger. It is sufficient to retain 11×11 terms in the series for deflection and 41×41 terms in the series for bending moments.

When the double trigonometric series is used to solve problems of the stress state of a smooth shell under the influence of a localized load, the number of significant terms sufficient to ensure the required degree of accuracy is much larger than the number necessary to solve an analogous problem for a ribbed shell with loads applied to the ribs. The presence of rib loads contributes to a substantial reduction and redistribution of strain and stress in the shell. The intensity of this effect increases with increasing stiffness of the ribs.

The results are in good agreement with the corresponding example in Khitrov,[6] shown in Fig. 3 and in Table 1.

Acknowledgment

The author wishes to thank Nahit Kumbasar for valuable help with this Technical Note.

References

[1] Şener, S., "Effect of Rib Eccentricity on Infinitely Long Cylindrical Shells," *ASCE Journal of Engineering Mechanics*, Vol. 119, No. 7, 1993, pp. 1493–1503.

[2] Flügge, W., *Stresses in Shells*, Springer–Verlag, New York, 1973.

[3] Ugural, A. C., *Stresses in Plates and Shells*, McGraw–Hill, New York, 1981.

[4] Şener, S., "On the Analysis of Ribbed Cylindrical Shell Reinforced with Stiffness in two Directions," Ph.D. Thesis, Istanbul Technical Univ., Istanbul, Turkey, 1983 (in Turkish).

[5] Şener, S., "Circular Cylindrical Shells with Reinforcing Ring," *International Symposium on Domes from Antiquity to the Present*, edited by I. Mungan, Mimar Sinan Univ., Istanbul, Turkey, 1988, pp. 445–452.

[6] Khitrov, V. N., "Determination of Strains and Stresses in a Shell Reinforced with Ribs in Two Directions," *Prikladnaya Mekhanika*, Vol. 7, No. 1, 1971, pp. 49–54 (English translation).

Extraction of Free-Free Modes Using Constrained Test Data

Ouqi Zhang* and Aspasia Zerva†
Drexel University, Philadelphia, Pennsylvania 19104

Nomenclature

$K_{xx}, K_{xy}, K_{yx}, K_{yy}$ = partitions of stiffness matrix corresponding to the fixed and unfixed degrees of freedom
M_{axx} = analytical mass matrix of constrained structure
$M_{xx}, M_{xy}, M_{yx}, M_{yy}$ = partitions of stiffness matrix corresponding to the fixed and unfixed degrees of freedom
m = number of measured modes used in the procedure
p_e = measured modal matrix of the constrained structure
p_{al}, p_{ah} = partitions of analytical modal matrix corresponding to lower and higher frequencies
p_{el}, p_{eh} = partitions of p_e corresponding to lower and higher frequencies
Ω_{ah} = diagonal matrix of analytical higher natural frequencies of the constrained structure
Ω_e = diagonal matrix of measured natural frequencies of the constrained structure
Ω_{el}, Ω_{eh} = partitions of Ω_e corresponding to lower and higher frequencies
ω = natural frequency of the unconstrained structure
$\|(\,)\|$ = sum of the squares of all elements of matrix ( )

Introduction

It is difficult to measure the mode shapes and frequencies of a vehicle that is unconstrained (free-free) by virtue of soft supports or suspensions. Przemieniecki[1] derived an analytical method for determining the modes of an unconstrained structure using the test data from the constrained ground vibration experiment. The method requires that all of the structural modes be measured, which is not possible in most cases for large aerospace structures. Recently, Chen et al.[2] proposed an approach to improve Przemieniecki's method by modal truncation so that only the lower modes need to be measured. However, the approach does not consider any compensation for the truncation of the higher modes.

In this Note, we present a method that considers the compensation for the modal truncation effect; it is essentially the application of the approach originally developed by Baruch and Bar Itzhack,[3] Wei,[4] Baruch,[5] and Berman and Nagy[6] for stiffness matrix modification.

Method of Przemieniecki and Chen et al.

The dynamic equation for a freely vibrating unconstrained system is given by

$$\left\{\begin{bmatrix} K_{xx} & K_{xy} \\ K_{yx} & K_{yy}\end{bmatrix} - \omega^2\begin{bmatrix} M_{xx} & M_{xy} \\ M_{yx} & M_{yy}\end{bmatrix}\right\}\begin{Bmatrix} q_x \\ q_y\end{Bmatrix} = 0 \tag{1}$$

in which the stiffness matrices K_{xx}, $K_{xy} = K^t_{yx}$, and K_{yy} are assumed to be obtained from static tests; the mass submatrices $M_{xy} = M^t_{yx}$ and M_{yy} are analytically derived; and the mode shapes are partitioned into q_x and q_y, respectively, corresponding to the unfixed and fixed degrees of freedom during the ground constrained test. Assuming that all modes of the constrained structure are measured from tests, Przemieniecki derived the relationship between the measured frequencies Ω_e and mode shapes p_e from the constrained test and the unknown mass submatrix M_{xx}

$$M_{xx} = K_{xx} p_e \Omega_e^{-2} p_e^{-1} \tag{2}$$

The term M_{xx} given by Eq. (2) can be substituted into Eq. (1) for the evaluation of the frequencies ω and mode shapes $\{q^t_x, q^t_y\}$ for the unconstrained system.

In Eq. (2), all of the frequencies and mode shapes are assumed to be measured from tests. To bypass this requirement, Chen et al.[2] partitioned Ω_e and p_e into lower and higher frequencies Ω_{el} and Ω_{eh} and modes p_{el} and p_{eh}, respectively, expressed M_{xx} by

$$M_{xx} = K_{xx} p_{el} \Omega_{el}^{-4} p^t_{el} K_{xx} + K_{xx} p_{eh} \Omega_{eh}^{-4} p^t_{eh} K_{xx} \tag{3}$$

Received May 24, 1995; revision received July 15, 1995; accepted for publication July 21, 1995.

*Research Assistant, Department of Civil and Architectural Engineering.
†Associate Professor, Department of Civil and Architectural Engineering.